Research Square

Preprints are preliminary reports that have not undergone peer review.
They should not be considered conclusive, used to inform clinical practice,
or referenced by the media as validated information.

Mechanism Study of ZNF468 Promoting Cervical Cancer Progression by Regulating the PI3K-AKT Signaling Pathway

Pengchen Xu
The Third People's Hospital of Bengbu Affiliated to Bengbu Medical University
Weichun Tang
The Third People's Hospital of Bengbu Affiliated to Bengbu Medical University
Ying Xu
The Third People's Hospital of Bengbu Affiliated to Bengbu Medical University
Qiang Li
Anhui Provincial Key Laboratory of Tumor Evolution and Intelligent Diagnosis and Treatment
Qian Chen
happy_sam01@sina.com

The Third People's Hospital of Bengbu Affiliated to Bengbu Medical University

Article

Keywords: Cervical cancer, ZNF468, proliferation, migration and invasion, PI3K-AKT signaling pathway

Posted Date: May 21st, 2026

DOI: https://doi.org/10.21203/rs.3.rs-9184565/v1

License: This work is licensed under a Creative Commons Attribution 4.0 International License.
Read Full License

Additional Declarations: No competing interests reported.

Abstract

Objective: To investigate the biological function of zinc finger protein ZNF468 in cervical cancer cells and its potential molecular mechanisms.

Methods: Western Blot analysis was performed to detect ZNF468 expression levels in HeLa, AV3, SiHa, and H8 cells. ZNF468 expression was knocked down in HeLa and AV3 cells using siRNA, with knockdown efficiency validated by RT-qPCR and Western Blot. Cell proliferation was assessed via CCK-8 assay, EdU staining, and colony formation assay. Cell migration and invasion were analyzed using scratch healing and Transwell assays. Downstream signaling pathways were screened using RNA-seq, and changes in key PI3K-AKT pathway proteins were detected by Western Blot.

Results: ZNF468 was highly expressed in both HeLa and AV3 cells. Knockdown of ZNF468 significantly inhibited proliferation, colony formation, migration, and invasion in cervical cancer cells. Mechanistic studies revealed that ZNF468 knockdown reduced PI3K and AKT phosphorylation levels, downregulated matrix metalloproteinase MMP9 expression, and simultaneously upregulated the epithelial marker E-cadherin.

Conclusion: ZNF468 promotes cervical cancer cell proliferation, migration, and invasion by activating the PI3K-AKT signaling pathway, suggesting its potential as a molecular target for cervical cancer therapy.

1. Introduction

Zinc finger proteins (ZNFs) constitute one of the largest transcription factor families in the human genome. They can specifically recognize and bind to DNA or RNA sequences, extensively participating in key biological processes such as gene transcription regulation, cellular signaling, and tumorigenesis. Consequently, they have become important targets in the study of molecular mechanisms underlying cancer [1–3]. Multiple studies indicate that abnormal expression or dysfunction of ZNF family members is closely associated with the proliferation, invasion, and metastasis of various malignant tumors, including lung cancer, liver cancer, and breast cancer [4–6]. As a member of this family, ZNF468 has been demonstrated to exert oncogenic effects in multiple tumors: in esophageal cancer, it promotes tumor cell proliferation and metastasis by activating the AURKA/PI3K/AKT pathway [7]; in breast cancer, it enhances tumor malignancy and induces chemotherapy resistance by upregulating TFAM expression [8]. However, the expression characteristics, biological functions, and associated molecular mechanisms of ZNF468 in cervical cancer remain unclear and warrant further systematic investigation.

Cervical cancer, as the most common malignant tumor of the female reproductive system, ranks among the leading causes of incidence and mortality among female malignancies worldwide [9–11]. Although HPV vaccination and the promotion of cervical cancer screening have significantly reduced its incidence, patients with advanced or recurrent disease still face severe challenges such as limited treatment options and poor prognosis [12, 13]. Therefore, in-depth analysis of the molecular regulatory networks

governing cervical cancer development and the identification of clinically valuable diagnostic biomarkers and therapeutic targets are crucial for improving patient outcomes.

Based on the above research background, this study focuses on the biological functions and mechanisms of ZNF468 in cervical cancer. First, Western Blot analysis was employed to detect expression differences of ZNF468 across various cervical cancer cell lines. Subsequently, siRNA technology was used to knock down ZNF468 expression in HeLa and AV3 cells. The impact of ZNF468 on malignant phenotypes of cervical cancer cells was systematically evaluated through CCK-8 assay, EdU proliferation analysis, colony formation assays, scratch healing assays, and Transwell migration/invasion assays. Finally, RNA-seq analysis was employed to identify potential downstream signaling pathways, with Western Blot validation of expression changes in key pathway-associated proteins. This study aims to elucidate the role of ZNF468 in cervical cancer progression and its underlying molecular mechanisms, thereby providing novel experimental evidence for targeted therapies against cervical cancer and expanding the application scope of zinc finger protein families in anti-tumor research.

2. Materials and methods

2.1. Materials

Human cervical cancer cells HeLa, AV3, and SiHa were purchased from Shanghai Saibai Kang Biotechnology Co., Ltd.; human cervical cancer cell line H8 was purchased from Shanghai Tongpai Biotechnology Co., Ltd.; MEM medium, DMEM/F12 medium, fetal bovine serum, and penicillin-streptomycin solution were purchased from Gibco; The CCK-8 assay kit was purchased from Japan's Dohin Chemical Laboratory; the EdU cell proliferation assay kit, crystal violet, paraformaldehyde, RIPA lysis buffer, and BCA protein concentration assay kit were all purchased from Shanghai Biyun Tian Biotechnology Co., Ltd.; Transwell chambers were purchased from Corning, USA; ZNF468 siRNA and negative control (NC) were purchased from Shanghai Jima Biotechnology Co., Ltd.; TRIzol reagent, reverse transcription kit, and qRT-PCR kit were purchased from TaKaRa; 2×RealStarPower SYBR qPCR Mix was purchased from Beijing Qingke Biotechnology Co., Ltd.; Lipofectamine 3000 transfection reagent was purchased from Invitrogen, USA; SDS-PAGE gel kit purchased from Beijing Solarbio Technology Co., Ltd.; ZNF468, PI3K, p-PI3K, AKT, p-AKT, MMP9, E-Cadherin, and GAPDH (internal control) antibodies, along with HRP-labeled goat anti-rabbit secondary antibody, all purchased from Hua'an Bio Co., Ltd.

2.2. Cell Culture and Transfection

Human cervical cancer cells HeLa and AV3 were cultured in MEM medium supplemented with 10% fetal bovine serum under standard conditions at 37°C in a 5% CO_2 incubator. Prior to experiments, HeLa and AV3 cells were seeded at appropriate densities into 6-well plates and cultured for 24 hours until 70–80% confluence was reached. Transfection was performed according to the Lipofectamine 3000 transfection reagent (Invitrogen) protocol. The experiment comprised three groups: a control group (NC, transfected

with non-targeted siRNA), and two ZNF468 knockdown groups (each containing two independent siRNA sequences: si-ZNF468-1 and si-ZNF468-2). After transfection, cells were cultured for an additional 48 hours before collection for subsequent experiments.

2.3. Western Blot detection of protein expression

After collection, cells were washed twice with pre-chilled PBS. The supernatant was removed by centrifugation, and RIPA lysis buffer was added. Lysis was performed on ice for 30 minutes. Subsequently, samples were centrifuged at 4°C and 12,000 g for 15 minutes. The supernatant was collected for protein concentration measurement. Subsequently, SDS-PAGE electrophoresis and membrane transfer were performed. The PVDF membrane was blocked with 5% nonfat milk. Primary antibodies (including ZNF468, PI3K, p-PI3K, AKT, p-AKT, MMP9, E-Cadherin, and the housekeeping control GAPDH antibody) and HRP-labeled secondary antibodies were incubated sequentially. Finally, the membrane was developed in a darkroom.

2.4. RT-qPCR detection of mRNA expression

Total RNA was extracted from HeLa and AV3 cells using TRIzol reagent. RNA integrity was verified by agarose gel electrophoresis. Following the reverse transcription kit protocol, total RNA was reverse transcribed into complementary DNA (cDNA). Using the cDNA as a template, quantitative real-time PCR was performed with 2×RealStarPower SYBR qPCR Mix. Reaction conditions were set as follows: 30-second pre-denaturation at 95°C, followed by 40 cycles of 5-second denaturation at 95°C and 30-second annealing-extension at 60°C. GAPDH served as the internal control gene. Relative expression levels of ZNF468 mRNA were calculated using the $2^{-\Delta\Delta CT}$ method. All experiments were independently replicated three times to ensure reliability of results.

2.5. CCK-8 Assay for Cell Viability

Transfected HeLa and AV3 cells were seeded at a density of 5×10^3 cells per well into 96-well plates, with six replicate wells per group. At 0, 24, 48, and 72 hours post-incubation, 10 μL of CCK-8 reagent was added to each well, followed by incubation at 37°C for 1 hour. Absorbance (OD values) was measured at 450 nm using a microplate reader. Finally, all groups were normalized against the NC group as a control to calculate cell proliferation rates.

2.6. EdU Assay for Cell Proliferation Capacity

Transfected HeLa and AV3 cells were seeded at appropriate densities in 12-well plates. After 48 hours of culture, EdU working solution (diluted according to kit instructions) was added to the wells and incubated at 37°C with 5% CO_2 for 2 hours. Subsequently, fixation, permeabilization, and staining steps were performed sequentially as per the kit manual. Cell nuclei were counterstained with DAPI. Under an inverted fluorescence microscope, five random fields of view were selected to count EdU-positive cells and total DAPI-stained cells, respectively. The EdU-positive cell rate (%) was calculated using the following formula: (EdU-positive cells / total cells)×100%.

2.7. Clonogenic Assay

Transfected HeLa and AV3 cells were seeded at a density of 1×10^3 cells per well in 6-well plates, with three replicate wells per group. After conventional culture for 14 days at 37°C and 5% CO_2, the medium was removed and the cells were washed twice with PBS. Cells were then fixed with 4% paraformaldehyde for 30 minutes and stained with crystal violet for 15 minutes. After staining, the plate was rinsed with running water and air-dried. Finally, images were captured, and the resulting clones were counted using ImageJ software.

2.8. Transwell Migration and Invasion Assay

Migration Assay: HeLa and AV3 cells, which were well-proliferating after transfection, were digested and centrifuged. They were then resuspended in serum-free MEM medium and counted. Cells were seeded at a density of 5×10^4 cells per well into the upper chamber of Transwell devices, while the lower chamber was filled with 700 μL of complete medium. After 24 hours of culture, the upper chamber was removed, and cells adhering to its inner surface were gently scraped off using a medical cotton swab. Cells were then fixed with 4% paraformaldehyde and stained with crystal violet. Residual crystal violet was washed away with PBS, and migrating cells were counted in five randomly selected fields of view under an inverted microscope.

Invasion assay: The upper chamber of the Transwell was pre-coated with Matrigel matrix gel (diluted 1:8). All other steps were identical to the migration assay. After 24 hours of incubation, the number of invading cells was counted.

2.9. Scratch Healing Assay

Well-grown HeLa and AV3 cells, following transfection, were seeded into 6-well plates. When confluence reached 90%, a straight line was scratched across the bottom of each well using a sterile 200 μL pipette tip. Cells were then washed twice with PBS to remove detached cells and cultured further in serum-free MEM medium. Scratch widths were photographed at 0 hours and 24 hours.

2.10. Transcriptome Sequencing

HeLa cells treated with siRNA transfection (NC group and ZNF468 knockdown group) were collected. Total RNA was extracted using the TRIzol method. mRNA was subsequently isolated and fragmented, followed by double-stranded cDNA synthesis, end repair, and library preparation. Samples were then sequenced. Raw sequencing data underwent bioinformatics analysis for quality control, gene expression quantification, and differential gene screening. Finally, differential genes were subjected to pathway enrichment analysis using the KEGG database.

2.11. Statistical Analysis

Data analysis was performed using SPSS 26.0 software. Multi-group comparisons employed one-way ANOVA, while pairwise comparisons utilized q-tests. $P < 0.05$ was considered statistically significant.

3. Results

3.1. Expression Levels of ZNF468 in Cervical Cancer Cell Lines

Western blot analysis revealed that ZNF468 exhibited higher expression levels in HeLa, AV3, and SiHa cells, while showing relatively lower expression in H8 cells (Fig. 1). To further investigate the function of ZNF468 in cervical cancer cells, we selected the HeLa and AV3 cell lines, which demonstrated higher expression levels, for subsequent functional and mechanistic studies.

3.2. Validation of ZNF468 siRNA Knockdown Efficiency

RT-qPCR results showed (Fig. 2A-B): Compared with the NC group, ZNF468 mRNA expression levels were significantly reduced in both HeLa and AV3 cells in the knockdown groups (ZNF468 siR-1, ZNF468 siR-2) ($P < 0.001$). Western blot results further confirmed (Fig. 2C-D) that ZNF468 protein expression in the knockdown groups was also lower than in the NC group. These findings indicate that both siRNAs exhibit robust interference effects and are suitable for subsequent experiments.

Note

(A, B) mRNA expression levels detected by RT-qPCR, (C, D) protein expression levels detected by WB; Compared with the NC group, $*P < 0.05$, $**P < 0.01$, $***P < 0.001$.

3.3. Effects of ZNF468 Knockdown on Cervical Cancer Cell Proliferation

CCK-8 assay results demonstrated significantly reduced proliferation rates in the knockdown group compared to the NC group at 24, 48, and 72 hours (Fig. 3A, B). EdU assay results revealed that the EdU-positive cell rate in the knockdown group was significantly lower than that in the NC group ($P < 0.001$) (Fig. 3C, D). The colony formation assay indicated that the number of colonies formed by knockdown group cells was significantly fewer than that in the NC group ($P < 0.01$) (Fig. 3E, F). Collectively, these results consistently demonstrate that ZNF468 knockdown significantly inhibits the proliferation and colony formation capabilities of cervical cancer cells.

Note

(A, B) CCK-8 proliferation curves; (C, D) EdU detection of cell proliferation and statistical analysis of positive cell rates; (E, F) Colony formation assays and statistical analysis of colony numbers. Compared with the NC group, $*P < 0.05$, $**P < 0.01$, $***P < 0.001$.

3.4. Effects of ZNF468 Knockdown on Migration, Invasion, and Wound Healing in Cervical Cancer Cells

Transwell migration assays revealed significantly fewer migrating cells in the knockdown group compared to the NC group ($P < 0.01$). Invasion assays demonstrated markedly reduced invasive cell numbers in the knockdown group relative to the NC group ($P < 0.001$) (Fig. 4A, B). The scratch healing assay indicated that the wound healing rate at 24 h was significantly lower in the knockdown group compared to the NC group (Fig. 4C, D). These results demonstrate that knocking down ZNF468 significantly inhibits the migration, invasion, and wound healing capacity of cervical cancer cells.

Note

(A, B) Transwell migration assay and migration cell count statistics, (C, D) Wound healing assay. Compared with the NC group, *$P < 0.05$, **$P < 0.01$, ***$P < 0.001$.

3.5. Transcriptome Sequencing Results

Through pathway and functional enrichment analysis of differentially expressed genes (Fig. 5A,B), results revealed significant enrichment of the PI3K-AKT signaling pathway following ZNF468 knockdown. This suggests ZNF468 may regulate biological processes such as cell proliferation and migration through this pathway.

Note

(A) Heatmap of differentially expressed genes after ZNF468 knockdown; (B) KEGG pathway enrichment diagram of differentially expressed genes after ZNF468 knockdown.

3.6. Effects of ZNF468 Knockdown on the PI3K-AKT Signaling Pathway in Cervical Cancer Cells

Western blot analysis revealed no significant changes in total PI3K and AKT protein levels in HeLa and AV3 cells following ZNF468 knockdown ($P > 0.05$). However, the levels of key pathway activation markers—phosphorylated PI3K (p-PI3K) and phosphorylated AKT (p-AKT)—were significantly reduced ($P < 0.001$). This indicates that ZNF468 knockdown specifically inhibits the activation of the PI3K-AKT signaling pathway without affecting the total expression of PI3K and AKT (Fig. 6A, B).

Note

(A) Expression of PI3K-AKT pathway-related molecules and grayscale values in HeLa cells after ZNF468 knockdown, (B) Expression levels and grayscale values of PI3K-AKT pathway-related molecules in AV3 cells after ZNF468 knockdown; Compared with the NC group, ns indicates no statistically significant difference ($P > 0.05$), *$P < 0.05$, **$P < 0.01$, ***$P < 0.001$.

3.7 Effects of ZNF468 Knockdown on Functional Molecules Downstream of the PI3K-AKT Pathway

To investigate the mechanism underlying phenotypic changes following PI3K-AKT pathway inhibition, we examined downstream proteins associated with cell invasion and epithelial-mesenchymal transition (EMT). Results demonstrated that ZNF468 knockdown significantly upregulated the expression of the epithelial marker E-cadherin while downregulating the expression of the invasion-related protein MMP9 ($P < 0.001$) (Fig. 7A, B). These findings suggest that ZNF468 may drive cervical cancer cell invasion and metastasis by activating the PI3K-AKT pathway, thereby suppressing E-cadherin expression and promoting MMP9 expression.

Note

(A) Expression levels and grayscale values of downstream molecules in the PI3K-AKT pathway in HeLa cells after ZNF468 knockdown; (B) Expression levels and grayscale values of downstream molecules in the PI3K-AKT pathway in AV3 cells after ZNF468 knockdown. Compared with the NC group, $*P < 0.05$, $**P < 0.01$, $***P < 0.001$.

4. Discussion

Zinc finger protein (ZNF) family members often exhibit context-dependent dual roles in tumor progression, functioning as both oncogenes and tumor suppressors in regulatory processes [14–16]. As a member of this family, ZNF468 has been reported to promote carcinogenesis in various malignancies including esophageal and breast cancers [7, 8, 14], yet its specific role and mechanisms in cervical cancer remain unclear. Therefore, this study systematically investigated the biological function of ZNF468 in cervical cancer for the first time. Experimental results demonstrated that knocking down ZNF468 significantly inhibited the proliferation, clonogenic formation, migration, and invasion capabilities of cervical cancer cells, suggesting that ZNF468 may act as an oncogenic factor in cervical cancer and participate in regulating tumor malignant progression.

At the mechanistic level, this study further explored the association between ZNF468 and the PI3K-AKT signaling pathway. Results demonstrated that knocking down ZNF468 significantly reduced the phosphorylation levels of p-PI3K and p-AKT, suggesting ZNF468 may function as an upstream regulator of this pathway. Abnormal activation of the PI3K-AKT pathway is a key driver of cervical cancer progression, typically associated with HPV E6/E7 oncoproteins or PIK3CA mutations [17–19]. This study first reveals that ZNF468 may represent a novel node regulating this pathway's activity. Concurrently, ZNF468 knockdown was accompanied by downregulation of MMP9 expression and upregulation of E-Cadherin expression. As a key enzyme in extracellular matrix degradation, elevated MMP9 expression is closely linked to enhanced tumor invasiveness [20, 21]; conversely, loss of E-cadherin expression is strongly associated with epithelial-mesenchymal transition (EMT) and cellular migration [22–24]. Collectively, these findings demonstrate that ZNF468 knockdown synergistically inhibits cervical cancer cell invasion and metastasis by suppressing PI3K-AKT pathway activation, upregulating E-Cadherin, and downregulating MMP9 expression. This further supports ZNF468's role as an upstream regulator in the PI3K-AKT pathway that promotes malignant progression in cervical cancer.

Based on the aforementioned mechanisms, ZNF468 holds promise as a novel therapeutic target for cervical cancer intervention. Its role as an upstream regulator offers new insights for developing combination treatment strategies. Additionally, ZNF468 expression levels may serve as a biomarker for auxiliary diagnosis or prognostic assessment, warranting further exploration. Of course, this study has certain limitations: the main conclusions are based on in vitro cell experiments, and future work should validate ZNF468's function in vivo by establishing cervical cancer xenograft models; the specific molecular mechanisms by which ZNF468 regulates the PI3K-AKT pathway (e.g., whether it directly transcriptionally regulates PIK3CA) require further clarification through experiments such as ChIP-qPCR and dual luciferase reporter assays; Furthermore, the potential interaction between ZNF468 and HPV infection, as well as the correlation between its expression levels and patient prognosis, require validation in larger-scale studies.

In summary, this study demonstrates that ZNF468 may promote cervical cancer cell invasion and metastasis by activating the PI3K-AKT signaling pathway, downregulating E-cadherin, and upregulating MMP9 expression. These findings provide experimental evidence supporting ZNF468 as a potential new therapeutic target for cervical cancer diagnosis and treatment.

Declarations

Ethics approval and consent to participate

This study exclusively utilized commercially available, established human cervical cancer cell lines (HeLa, AV3, SiHa, and H8) purchased from certified biotechnology companies (Shanghai Saibai Kang Biotechnology Co., Ltd. and Shanghai Tongpai Biotechnology Co., Ltd.). No human participants, primary human tissues, or animals were involved in this research; therefore, ethical approval and informed consent were not required.

Consent for publication

Not applicable. This manuscript does not contain any individual person’s data or identifiable images.

Competing interests

The authors declare that they have no competing interests.

Ethics Statement

The data used in this study are publicly available and permitted for unrestricted reuse under an open license.

Conflict of interest statement

The authors declare no conflict of interest, financial or otherwise.

Funding statement

This work was supported by the Open Project of Anhui Provincial Key Laboratory of Tumor Evolution and Intelligent Diagnosis and Treatment (No. KFKT202413), the Bengbu Science and Technology Innovation Guidance Project (No. 2024ZD0049),the Key Natural Science Research Project of Anhui Provincial Education Department(No.2025AHGXZK31548).

Author Contribution

PX contributed to data analysis and manuscript preparation. WT and YX performed the in vitro experiments. QL and QC conceived and designed the study and critically revised the manuscript. All authors reviewed, edited, and approved the final manuscript, and agreed to be accountable for the accuracy and integrity of the work.

Acknowledgments

Thank all authors for their contributions to this study.

Data Availability

The datasets generated and analysed during the current study are available in the [NCBI] repository, [https://submit.ncbi.nlm.nih.gov/subs/ ACCESSION NUMBER TO DATASETS PRJNA1418263]

References

1. Laity, J. H., Lee, B. M. & Wright, P. E. Zinc finger proteins: new insights into structural and functional diversity[J]. *Curr. Opin. Struct. Biol.* **11** (1), 39–46 (2001).
2. Peng, W. et al. Zinc finger protein 82 regulates p53 protein stability through histone deacetylase and enhances neo-adjuvant chemotherapy in esophageal cancer[J]. *Cell Death Dis.* **16** (1), 694 (2025).
3. Cai, A. et al. Downregulation of KRAB zinc finger proteins in 5-fluorouracil resistant colorectal cancer cells[J]. *BMC Cancer*. **22** (1), 596 (2022).
4. Zhang, Y. et al. ZNF451 favors triple-negative breast cancer progression by enhancing SLUG-mediated CCL5 transcriptional expression[J]. *Cell. Rep.* **42** (6), 112654 (2023).
5. Zhang, H. et al. ZNF740 facilitates the malignant progression of hepatocellular carcinoma via the METTL3/HIF-1A signaling axis[J]. *Int. J. Oncol.* **65** (5), 105 (2024).

6. Zhang, X. et al. ZNF452 facilitates tumor proliferation and invasion via activating AKT-GSK3β signaling pathway and predicts poor prognosis of non-small cell lung cancer patients[J]. *Oncotarget* **8** (24), 38863–38875 (2017).
7. Bai, G. et al. ZNF468/AURKA/PI3K/AKT positive feedback loop promotes proliferation and metastasis of oesophageal squamous cell carcinoma[J]. *J. Cell. Mol. Med.* **29** (14), e70724 (2025).
8. Jia, Z. et al. Zinc finger protein 468 up-regulation of TFAM contributes to the malignant growth and cisplatin resistance of breast cancer cells[J]. *Cell Div.* **19** (1), 8 (2024).
9. Sung, H. et al. Global cancer statistics 2020: GLOBOCAN estimates of incidence and mortality worldwide for 36 cancers in 185 countries[J]. *Cancer J. Clin.* **71** (3), 209–249 (2021).
10. Azangou-Khyavy, M. et al. Global, regional, and national quality of care index of cervical and ovarian cancer: a systematic analysis for the global burden of disease study 1990–2019[J]. *BMC Womens Health*. **24** (1), 69 (2024).
11. Li, Z. et al. Global landscape of cervical cancer incidence and mortality in 2022 and predictions to 2030: The urgent need to address inequalities in cervical cancer[J]. *Int. J. Cancer*. **157** (2), 288–297 (2025).
12. Soares, D. et al. Immunotherapy in cervical and endometrial cancer: current landscape and future directions[J]. *Life (Basel Switzerland)*. **14** (3), 334 (2024).
13. Galicia-Carmona, T. et al. Advanced, recurrent, and persistent cervical cancer management: in the era of immunotherapy[J]. *Front. Oncol.* **14**, 1392639 (2024).
14. Ye, L. et al. Overexpression of ZNF468 promotes esophageal squamous cell carcinoma progression via the AKT/mTOR pathway[J]. *Int. Immunopharmacol.* **143** (Pt 3), 113509 (2024).
15. Liu, S. et al. Zinc finger proteins in the war on gastric cancer: molecular mechanism and clinical potential[J]. *Cells* **12** (9), 1314 (2023).
16. Iyer, A. S. et al. The Roles of Zinc Finger Proteins in Colorectal Cancer[J]. *Int. J. Mol. Sci.* **24** (12), 10249 (2023).
17. Bossler, F., Hoppe-Seyler, K. & Hoppe-Seyler, F. PI3K/AKT/mTOR Signaling Regulates the Virus/Host Cell Crosstalk in HPV-Positive Cervical Cancer Cells[J]. *Int. J. Mol. Sci.* **20** (9), 2188 (2019).
18. Jiang, W. et al. The PIK3CA E542K and E545K mutations promote glycolysis and proliferation via induction of the β-catenin/SIRT3 signaling pathway in cervical cancer[J]. *J. Hematol. Oncol.* **11** (1), 139 (2018).
19. Wang, Y. et al. Integrated genomic and transcriptomic analysis reveals the activation of PI3K signaling pathway in HPV-independent cervical cancers[J]. *Br. J. Cancer*. **130** (6), 987–1000 (2024).
20. Umemoto, K. et al. Platelets and MMP 9 contribute to esophageal cancer invasion via CD40 CD154 interactions[J]. *Oncol. Rep.* **54** (1), 79 (2025).
21. Sai, X. B. et al. TSG101, a tumor susceptibility gene, bidirectionally modulates cell invasion through regulating MMP-9 mRNA expression[J]. *BMC Cancer*. **15**, 933 (2015).

22. Bae, G. Y. et al. Loss of E-cadherin activates EGFR-MEK/ERK signaling, which promotes invasion via the ZEB1/MMP2 axis in non-small cell lung cancer[J]. *Oncotarget* **4** (12), 2512–2522 (2013).
23. Onder, T. T. et al. Loss of E-cadherin promotes metastasis via multiple downstream transcriptional pathways[J]. *Cancer Res.* **68** (10), 3645–3654 (2008).
24. Kondo, K. et al. E/N-cadherin switch mediates cancer progression via TGF-β-induced epithelial-to-mesenchymal transition in extrahepatic cholangiocarcinoma[J]. *Br. J. Cancer*. **105** (12), 1885–1893 (2011).

Figures

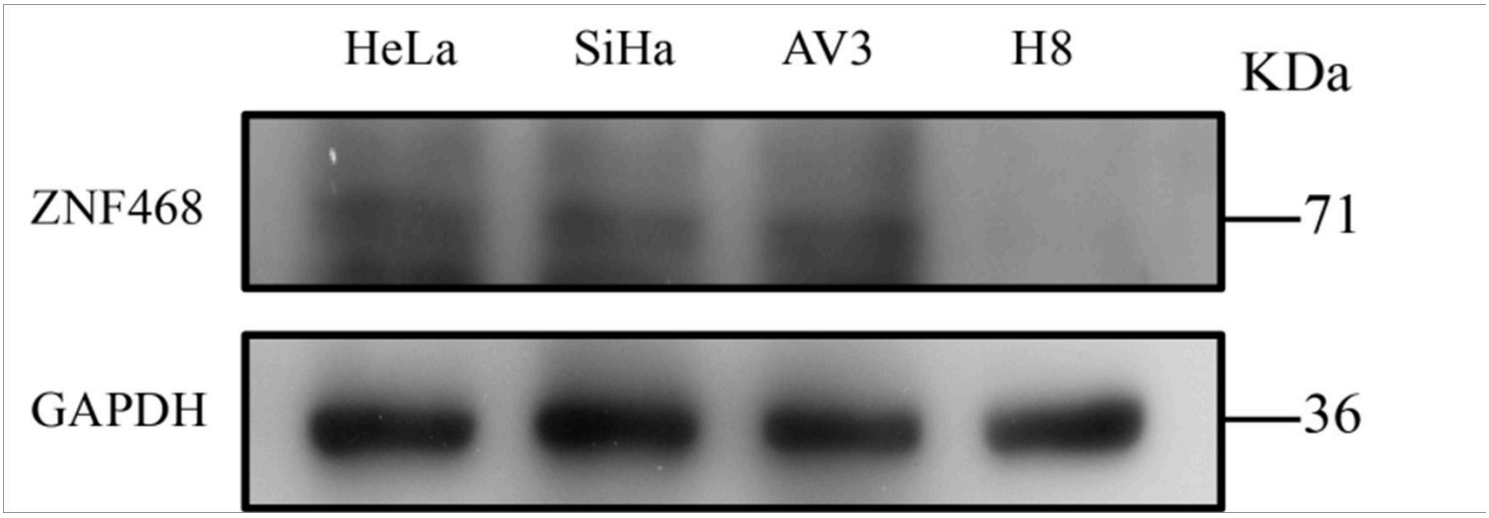


Figure 1

Expression Levels of ZNF468 in Cervical Cancer Cell Lines

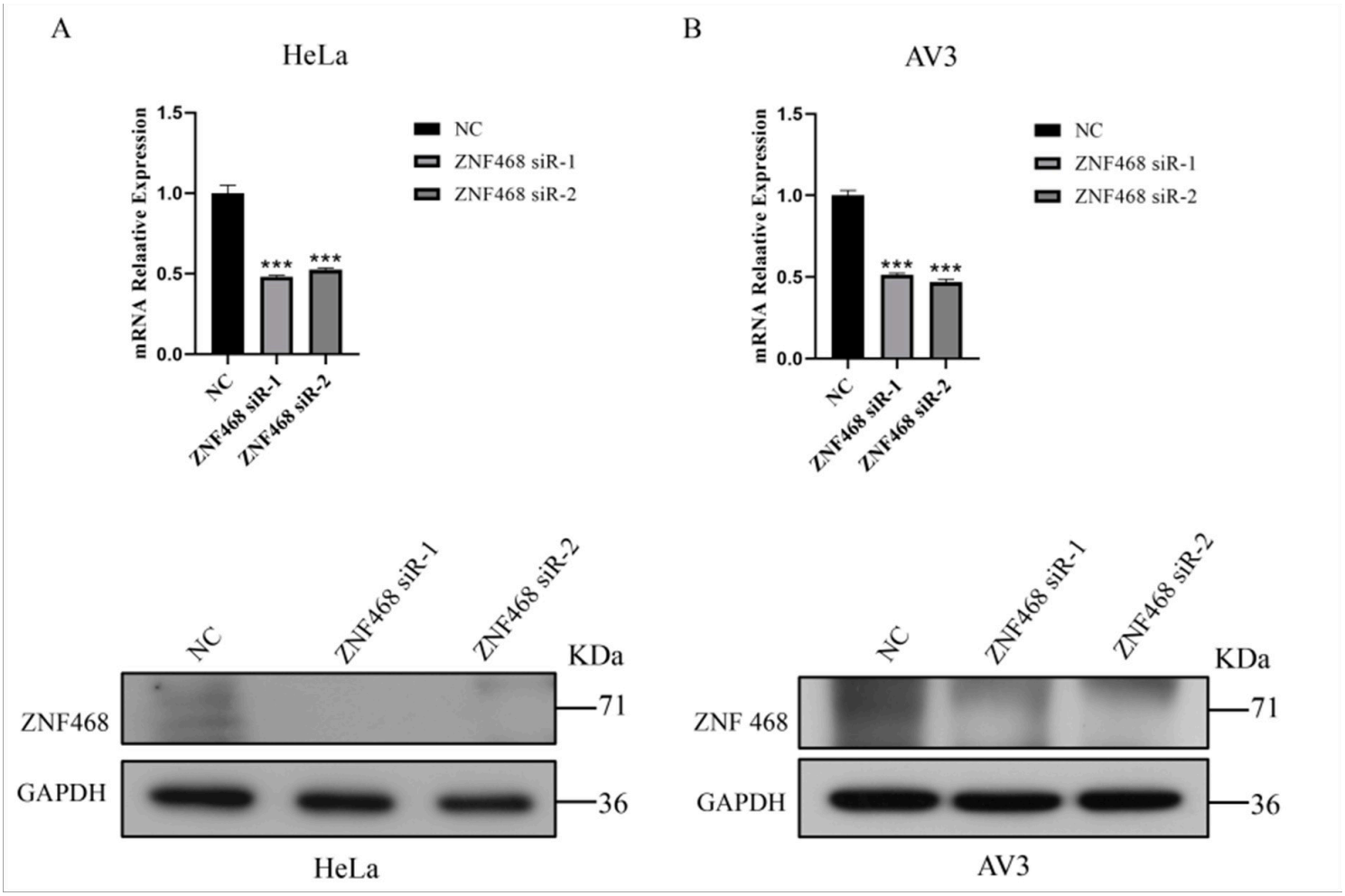


Figure 2

Inhibition of ZNF468 Expression by siRNA-ZNF468 in HeLa and AV3 Cells

Note: (A, B) mRNA expression levels detected by RT-qPCR, (C, D) protein expression levels detected by WB; Compared with the NC group, *$P < 0.05$, **$P < 0.01$, ***$P < 0.001$.

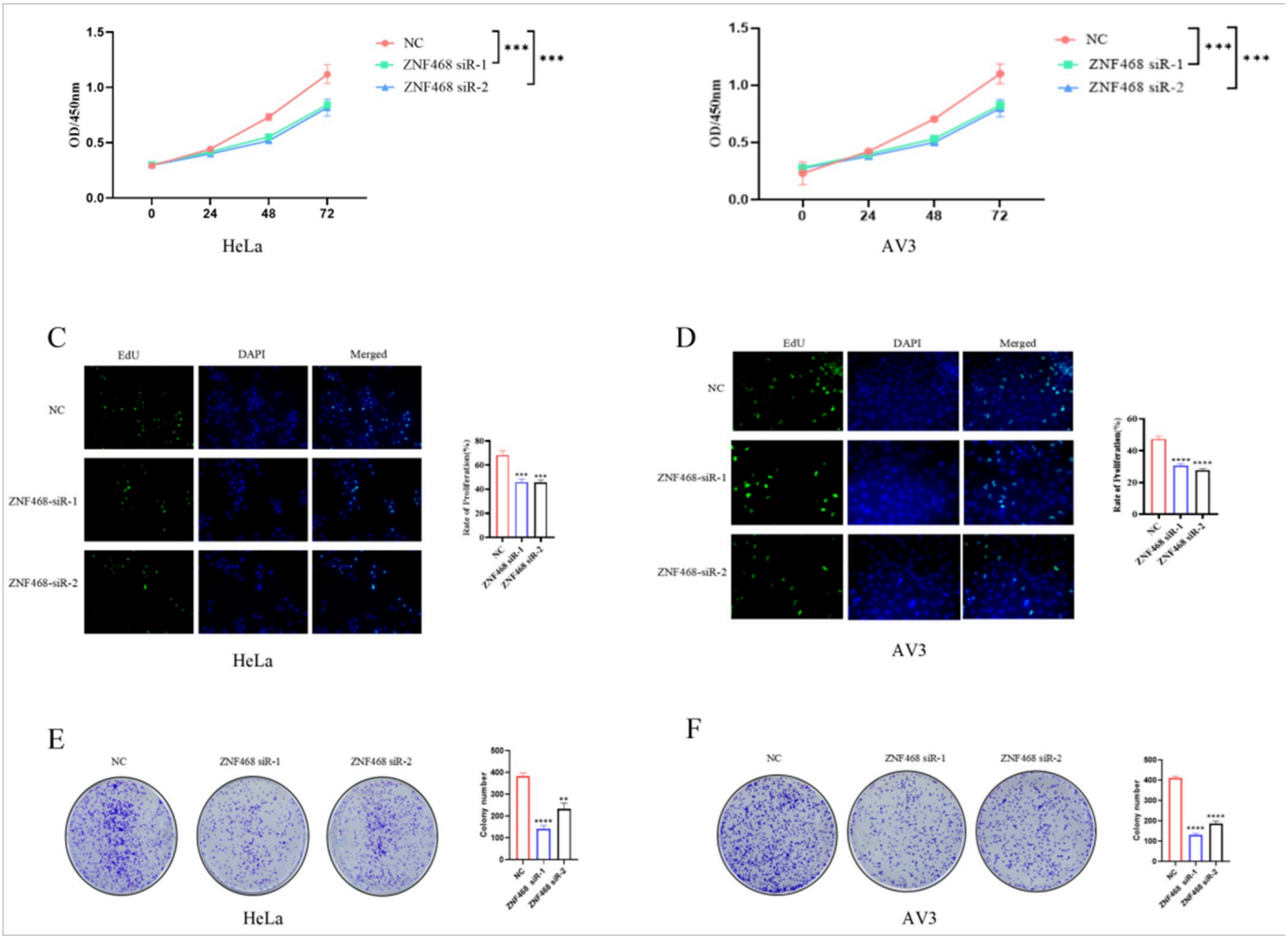
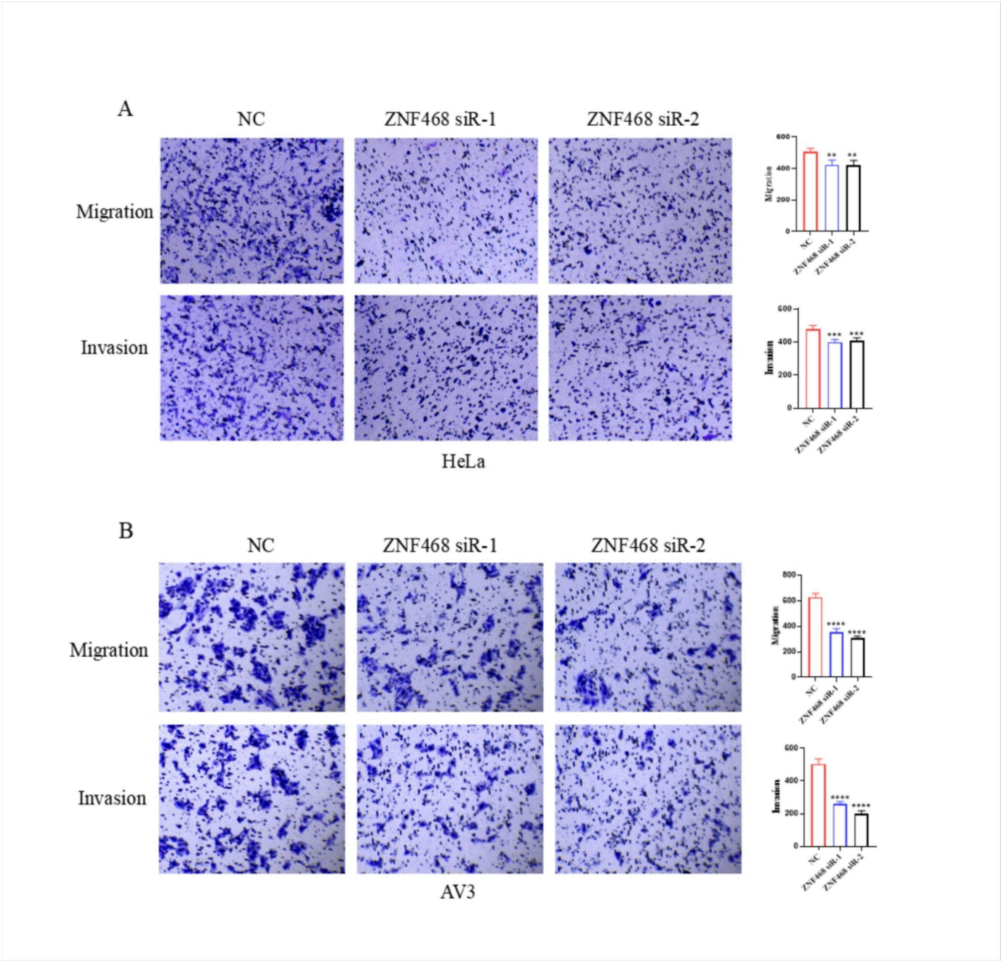


Figure 3

Effects of ZNF468 Knockdown on Proliferation and Colony Formation in HeLa and AV3 Cells

Note: (A, B) CCK-8 proliferation curves; (C, D) EdU detection of cell proliferation and statistical analysis of positive cell rates; (E, F) Colony formation assays and statistical analysis of colony numbers. Compared with the NC group, *$P < 0.05$, **$P < 0.01$, ***$P < 0.001$.



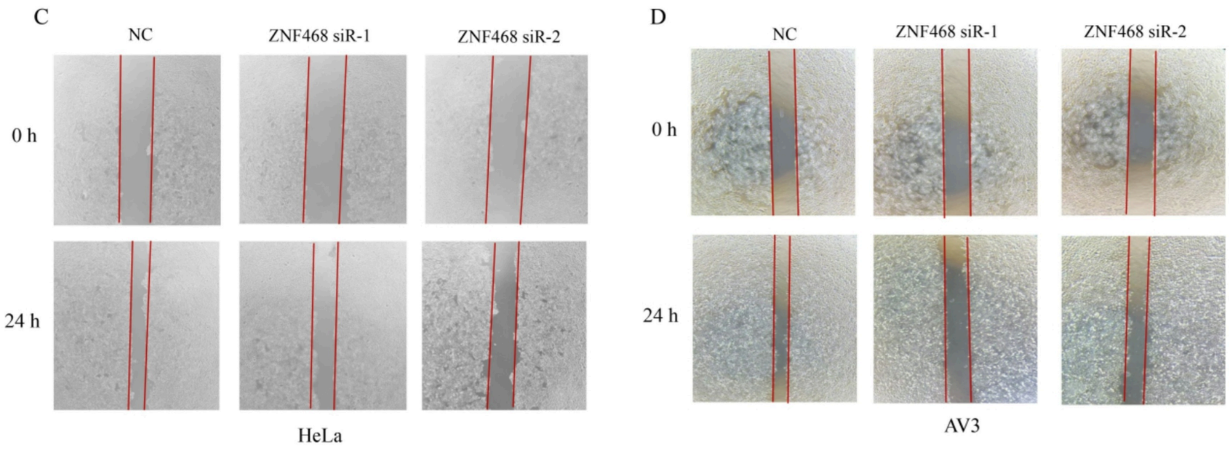


Figure 4

Effects of ZNF468 Knockdown on Migration, Invasion, and Wound Healing in HeLa and AV3 Cells

Note: (A, B) Transwell migration assay and migration cell count statistics, (C, D) Wound healing assay. Compared with the NC group, *P< 0.05, **P < 0.01, ***P < 0.001.

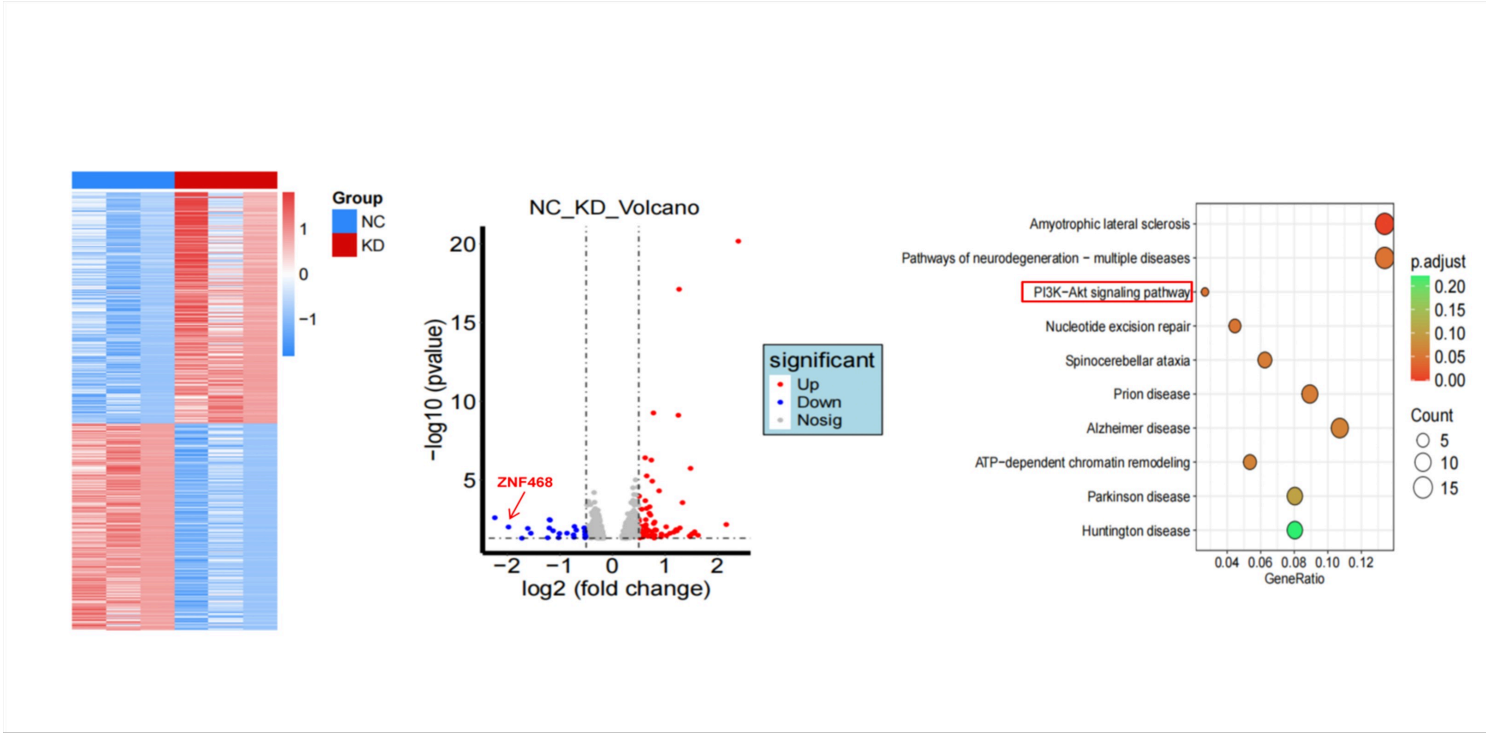


Figure 5

Transcriptome sequencing results after ZNF468 knockdown

Note: (A) Heatmap of differentially expressed genes after ZNF468 knockdown; (B) KEGG pathway enrichment diagram of differentially expressed genes after ZNF468 knockdown.

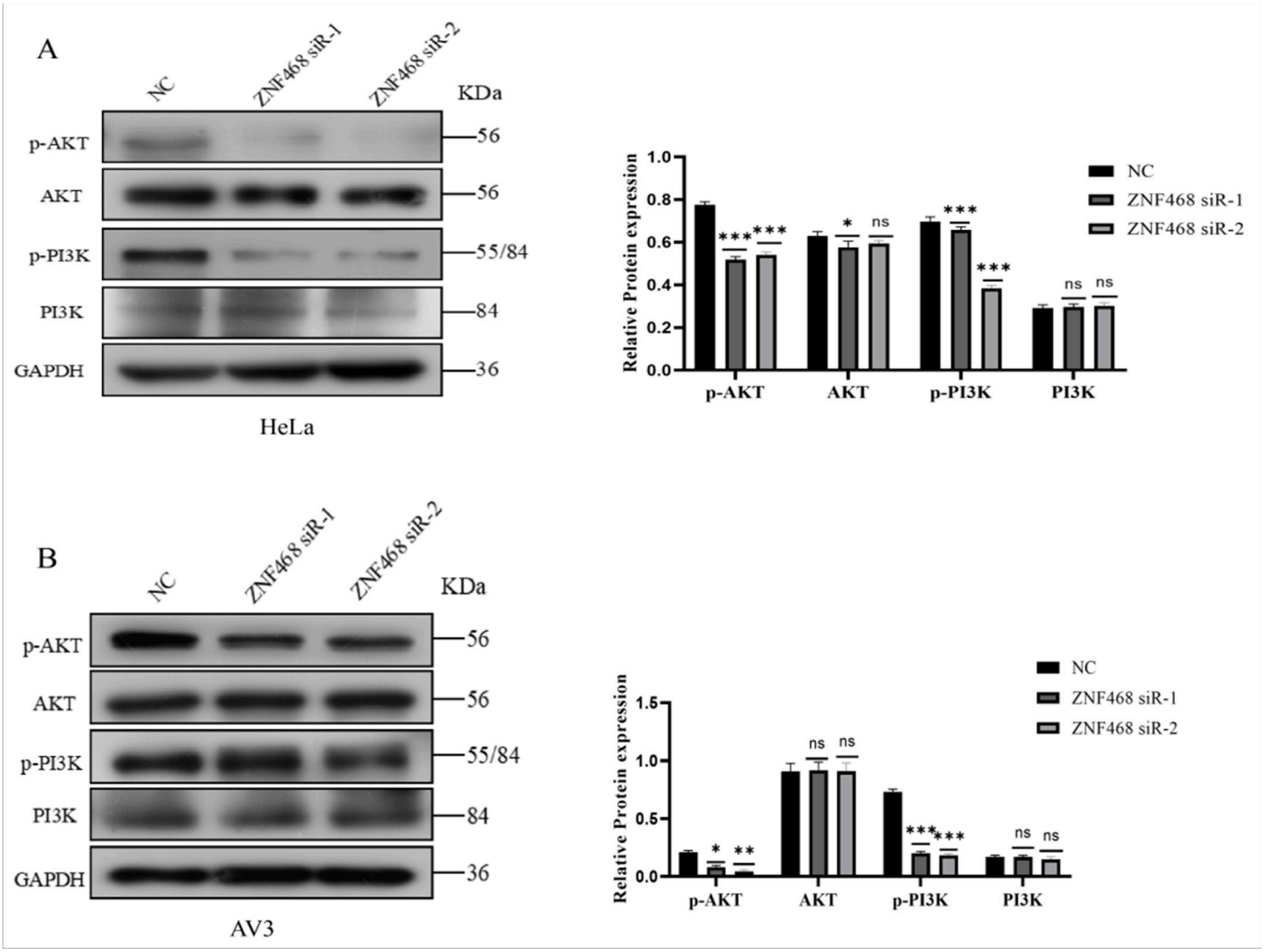


Figure 6

ZNF468 regulates cervical cancer cell functions via the PI3K-AKT signaling pathway

Note: (A) Expression of PI3K-AKT pathway-related molecules and grayscale values in HeLa cells after ZNF468 knockdown, (B) Expression levels and grayscale values of PI3K-AKT pathway-related molecules in AV3 cells after ZNF468 knockdown; Compared with the NC group, ns indicates no statistically significant difference ($P > 0.05$), *$P < 0.05$, **$P < 0.01$, ***$P < 0.001$.

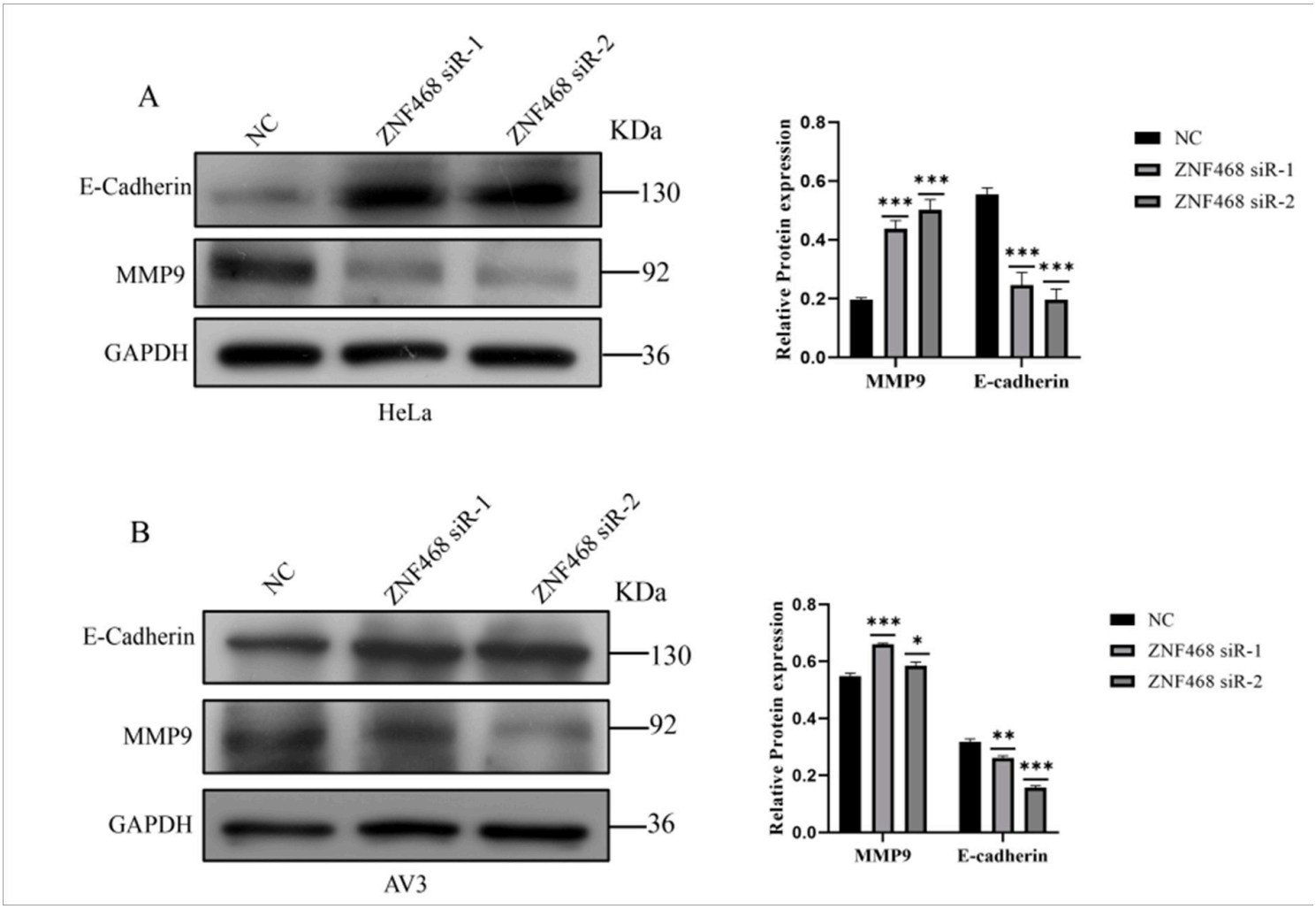


Figure 7

Effects of ZNF468 Knockdown on Downstream Functional Molecules of the PI3K-AKT Pathway

Note: (A) Expression levels and grayscale values of downstream molecules in the PI3K-AKT pathway in HeLa cells after ZNF468 knockdown; (B) Expression levels and grayscale values of downstream molecules in the PI3K-AKT pathway in AV3 cells after ZNF468 knockdown. Compared with the NC group, **P* < 0.05, ***P* < 0.01, ****P* < 0.001.